

Determination of Transverse Vibrations in a Curved Building through Wind Tunnel Testing

Carlos M. Walter

¹Professor,

Department of Physics,

Faculty Of Engineering, Universidad Nacional del Comahue, Neuquén, Argentina.

Corresponding Author: Carlos M. Walter.

ABSTRACT

This study investigates wind-induced vibrations in curved buildings through wind tunnel experimentation. An circular arc airfoil model is used, whose shape is common in buildings. Initially, a 12% circular arc roof is studied, positioned horizontally with respect to the wind flow direction. Then, a curved building with a 32% circular arc airfoil is analyzed, positioned vertically relative to the wind direction, considering the presence of the atmospheric boundary layer. The atmospheric boundary layer is modeled in the wind tunnel of the Environmental Fluid Dynamics Laboratory (LaDiFA) of the Faculty of Engineering at Universidad Nacional del Comahue. The experimental method consists of video recording the displacements at different wind attack angles. From these recordings, a spectral analysis is performed to determine dominant frequencies. Through these frequencies, and by means of Strouhal number similarity, results are extrapolated from the model to the prototype. The obtained results allow the identification of characteristic frequencies associated with different wind angles of attack, providing relevant information about the behavior of both the model and the prototype under vibration. These data constitute a basis for comparing measured frequencies with those of a real structure and evaluating the potential impact of wind on it.

KEYWORDS: *Vibration, Wind Tunnel, Strouhal Number.*

Date of Submission: 07-04-2026

Date of acceptance: 20-04-2026

I. INTRODUCTION

Contemporary architecture increasingly explores unconventional geometries aimed at enhancing both aesthetics and aerodynamic performance. Among these, curved buildings represent a particularly innovative and challenging structural typology. Due to their aerodynamic shape, such structures are subject to lift and drag forces analogous to those experienced by airfoils. These forces are highly sensitive to the angle of attack and, consequently, to wind direction. This sensitivity introduces complex flow-structure interactions that must be carefully evaluated to ensure both structural integrity and occupant comfort.



Figure: 1.1. DLF Gateway Tower, circular arc airfoil building, Gurugram, India

The CIRSOC 102 standard “Wind Action on Structures” of Argentina [1] (based on the ASCE 7 standard) recommends the use of wind tunnel testing for buildings with unconventional geometries, as such configurations do not satisfy the regularity assumptions required by the analytical procedures prescribed in the code. Wind tunnel testing constitutes a fundamental experimental tool for analyzing airflow behavior around structures through the use of scaled models. By measuring surface pressures and the surrounding wind velocity field, and applying similarity principles, it is possible to accurately predict the aerodynamic behavior of the full-scale prototype. The design of this type of wind tunnel consists of a rectangular test section with fixed dimensions that remain constant over a specified length. At one end, an electric motor with a fan is installed to draw air through the tunnel. At the opposite end, the air inlet has a convergent shape. A grid is placed at this inlet to stabilize potential vortex shedding as the flow enters the wind tunnel. Downstream, within the constant-section test area, vortex generators and floor roughness elements are installed to reproduce the wind profile with the appropriate level of turbulence (Figure 1.2).

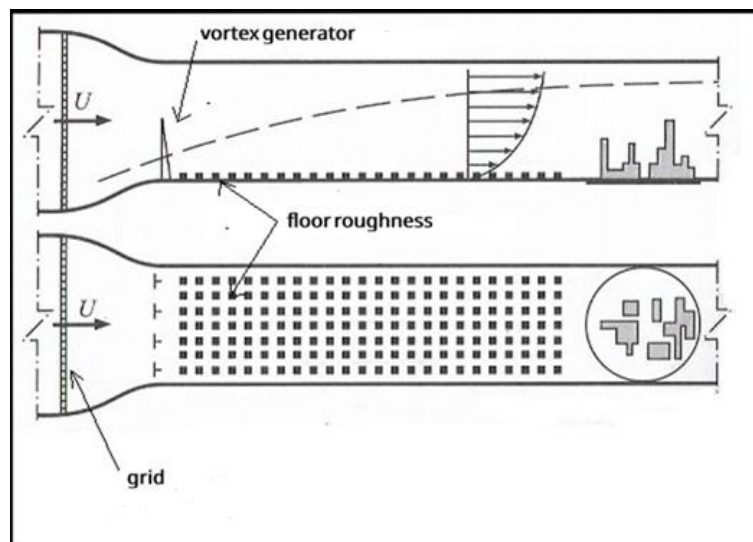


Figure: 1.2. Schematic of the boundary layer wind tunnel, where vortex generators and floor roughness elements are adjusted to reproduce the atmospheric boundary layer, adapted from Meseguer et al. (2001) [2].

II. METHODOLOGY

Model Formulation

The prototype considered in this study is a curved building with a circular arc airfoil of 32% thickness, representative of a group of buildings located in Cipolletti, Río Negro, Argentina. While these buildings share similar cross-sectional geometry, they differ in height. The tallest structure (height = 60 m; width = 30 m; thickness = 9.6 m) is selected for analysis.





Figure: 2.1. Prototype: buildings with circular arc profiles, Cipolletti, Río Negro, Argentina.

A scale model (1:250) is constructed, with dimensions: height = 0.24 m, width = 0.12 m, and thickness = 0.0384 m.

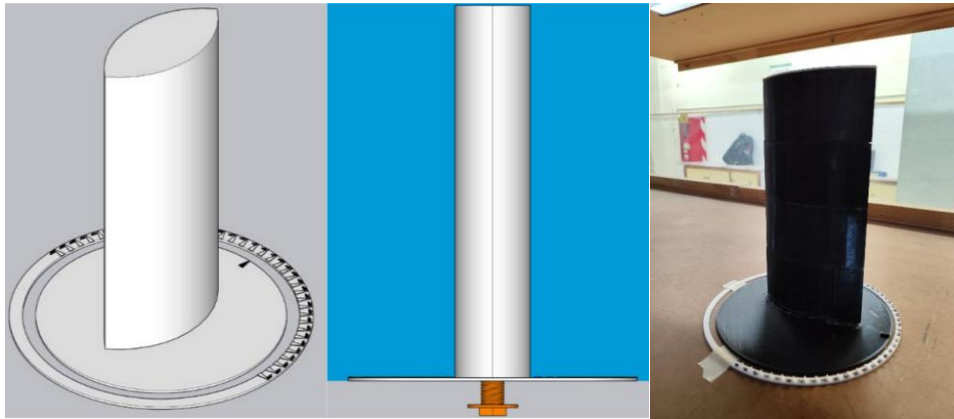


Figure: 2.2. 3D model schematic. Photograph of the model in the wind tunnel test section.

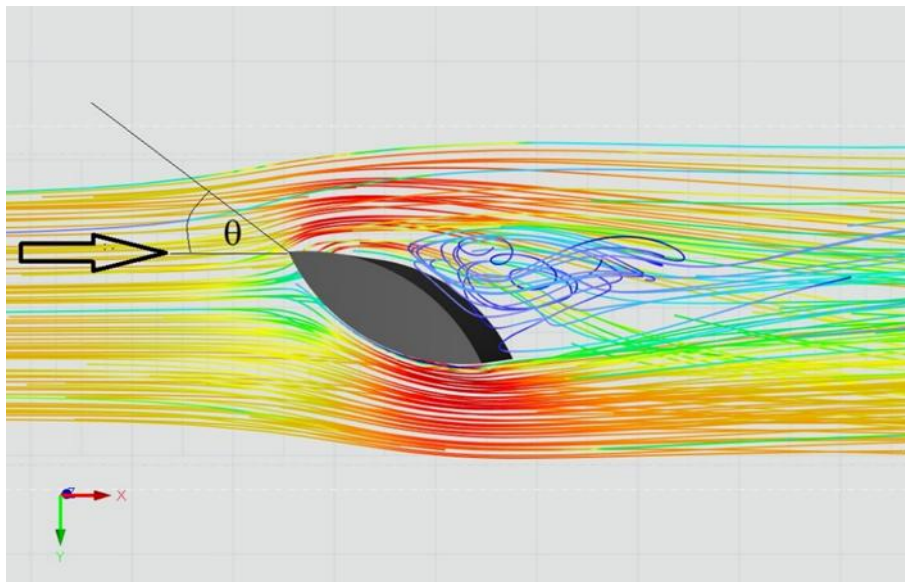


Figure: 2.3. Building model at different angles of attack.

Determination of Transverse Vibrations in a Curved Building under Wind Loading

Wind-induced vibrations are critical not only due to their potential to cause structural damage but also because of their impact on occupant comfort. Even when structural safety is not compromised, excessive oscillations may lead to serviceability issues.

Structures exposed to atmospheric wind are subjected to three primary types of loading: along-wind loads (drag forces), across-wind loads, caused by periodic vortex shedding and torsional loads, due to asymmetric pressure distributions.

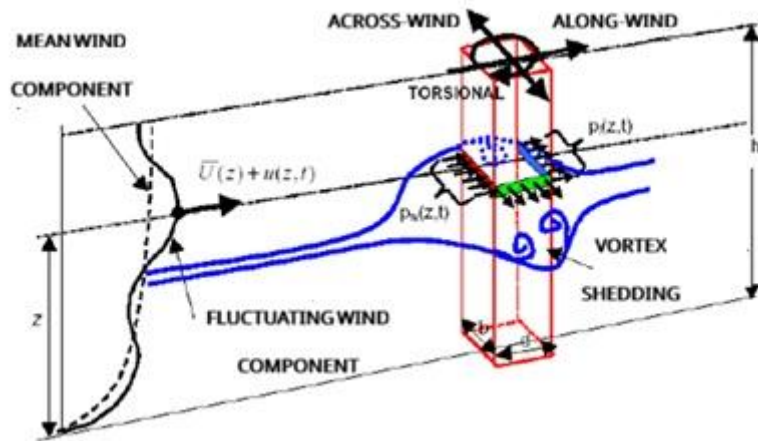


Figure: 2.4. Schematic of wind-induced loads acting on a structure.

For stiff reinforced concrete structures, a quasi-static approach is often sufficient. However, in more flexible systems, dynamic effects become significant. Three coupled phenomena may arise: resonance, when structural natural frequencies coincide with vortex shedding frequencies; flutter, an aeroelastic instability involving coupling between bending and torsion; and inertial amplification, where increased displacements lead to dominant inertial forces.

The Strouhal Number

The Strouhal number (St) is a dimensionless parameter that relates vortex shedding frequency to flow velocity and a characteristic length:

$$St = \frac{L \cdot Fc}{V}$$

St: Strouhal number

L: Structural diameter or distance between the edges where separation occurs

V: Wind velocity

Fc: Frequency of vortex shedding

The Strouhal number plays a key role in scaling experimental results and predicting aerodynamic behavior.

Knisely (1990) [3] makes a literature review about the Strouhal number in cylinders of rectangular and square base, and with wind tunnel tests provides new data in this regard. Figures 2.5 and 2.6 shows the variation of the number of Strouhal as a function of the angle of attack of the wind on a cylindrical body of square base, where it is observed that for angles between 0° and 12° there is a linear increasing variation of the St , then it remains constant up to 78° and decays to 90° (there is a symmetry from 45° to 90°).

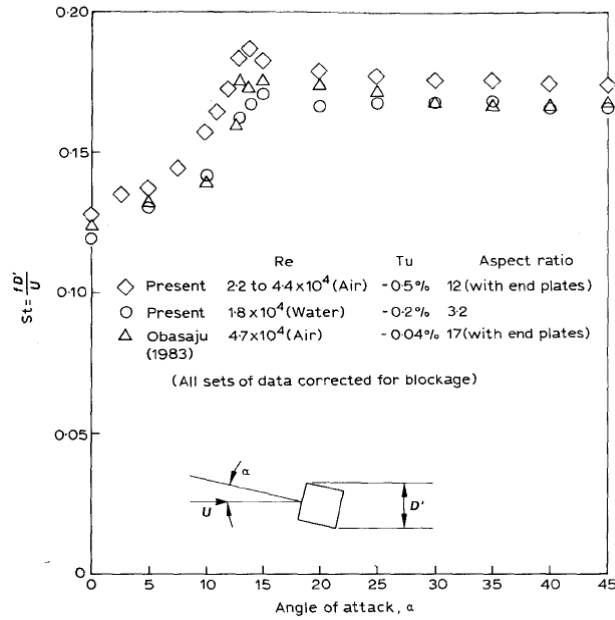


Figure: 2.5. Variation of the Strouhal number with angle of attack (adapted from Knisely, 1990).

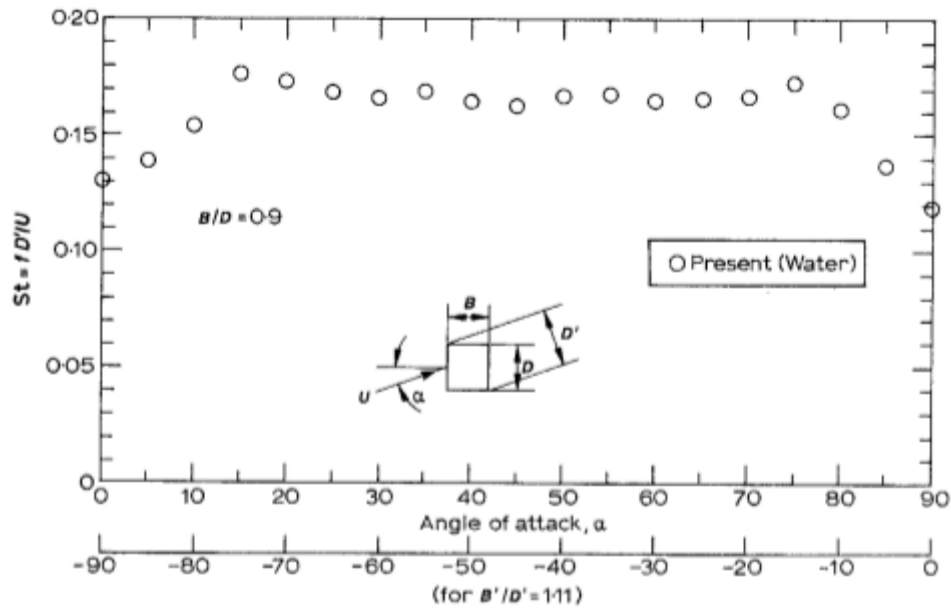


Figure: 2.6. Strouhal number as a function of the angle of attack for $B/D = 0.9$ (adapted from Knisely, 1990).

Vortex Shedding in Curved Buildings

Unlike sharp-edged bodies, vortex shedding in curved structures is governed by boundary layer separation induced by adverse pressure gradients. Consequently, their behavior resembles that of streamlined aerodynamic profiles rather than bluff bodies.

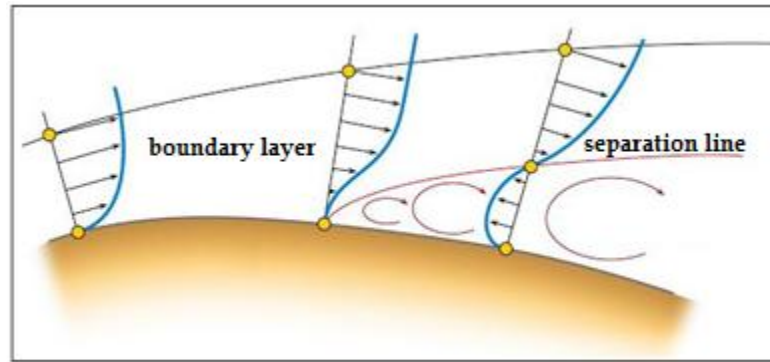


Figure: 2.7. Separation of boundary layer.

Therefore, this type of vortex shedding is expected to resemble more closely the behavior observed in aerodynamic profiles rather than that reported by Knisely (1990). Accordingly, relevant literature on vortex shedding in symmetric aerodynamic profiles of the NACA 00XX type was considered, such as the study conducted by Yarusevych and Boutilier (2010) [4]. For Reynolds numbers on the order of 1.5×10^5 , Strouhal numbers were found to be approximately equal to 1. Yarusevych et al. (2009) [5] investigated the wake of a NACA 0025 airfoil and concluded that, for angles of attack between 0° and 10° , the Strouhal number increases with increasing Reynolds number within the range of 5×10^4 to 1.5×10^5 , and then remains approximately constant. On the other hand, Mahbub Alam et al. (2010) [6] observed, for a NACA 0012 airfoil, that the Strouhal number depends on the angle of attack of the flow over the profile, while remaining nearly constant for Reynolds numbers between 1×10^4 and 6×10^4 . In the study by Walter and Lässig (2018) [7], a series of wind tunnel experiments was conducted using a circular-arc airfoil (with a thickness of 20%) as a first approach to determine how the Strouhal number varies with the angle of attack. The airfoil was arranged horizontally, in a configuration analogous to a wing. These types of airfoils are commonly used in architectural applications such as curved buildings, airport roofs, and bus terminals.

The experiments were carried out for Reynolds numbers between 6×10^4 and 1×10^5 . Velocity measurements were taken in the wake at the point defined by the coordinates $Y = 3.5 \cdot C$ (three and a half times the chord length), $X = 0.4 \cdot C \cdot \sin(\alpha)$ (four-tenths of the chord length multiplied by the sine of the angle of attack), as schematically shown in Figure 2.8.

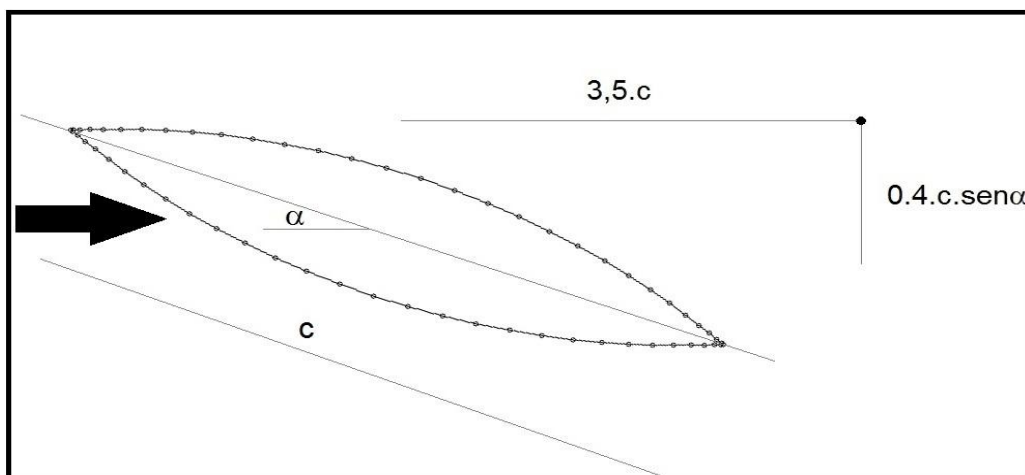


Figure: 2.8. Profile dimensions and location of the vortex shedding measurement point.

Tests were conducted at angles of attack ranging from 0° to 30° in 5° increments, and from 30° to 90° in 15° increments. Figures 2.9 and 2.10 illustrates two examples of the frequency spectra obtained.

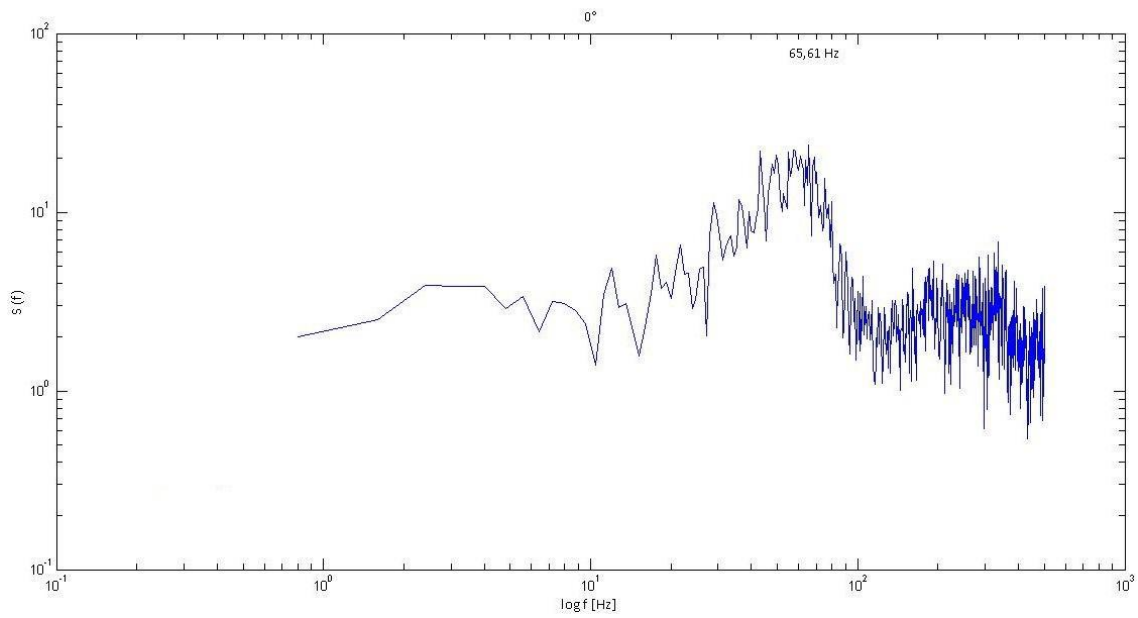


Figure: 2.9. Power spectral density. Peak of 65.61 Hz at $\alpha = 0^\circ$.

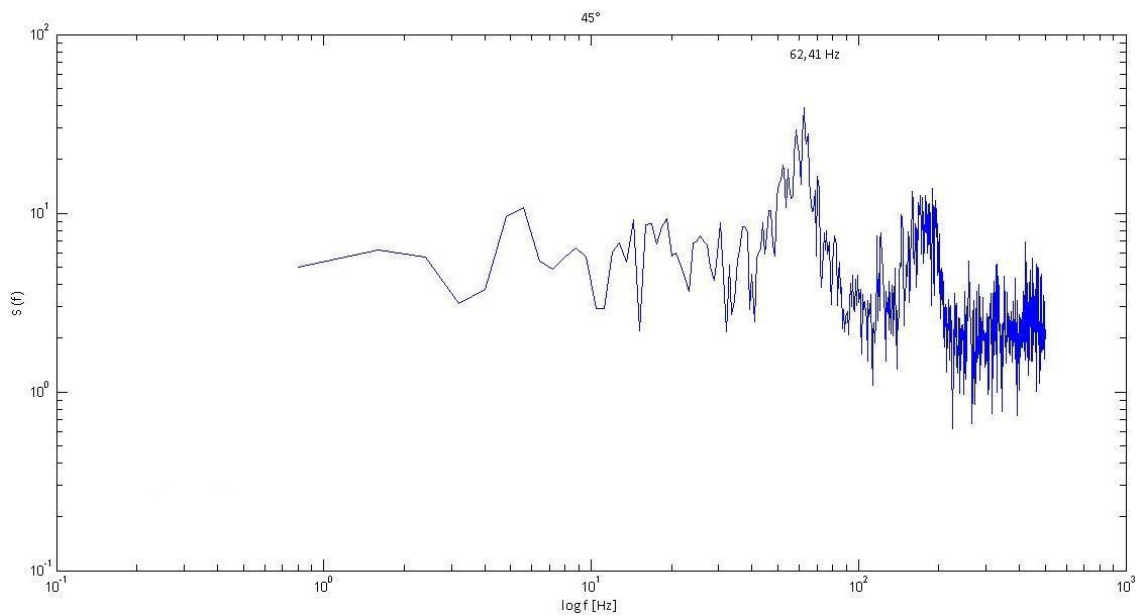


Figure: 2.10. Power spectral density. Same peak at 62.41 Hz at 45° and 60° .

The primary vortex shedding frequency was analyzed, and the corresponding Strouhal number was calculated as a function of the angle of attack. The results are presented in Figure 2.11

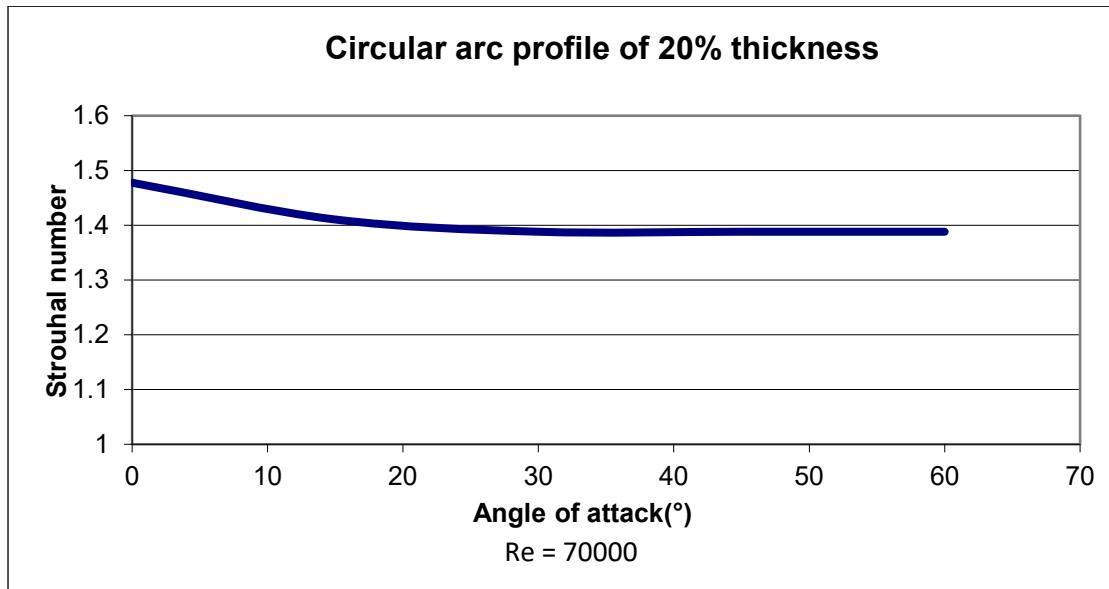


Figure: 2.11. Variation of Strouhal number with the angle of attack in a circular arc airfoil (20% thickness) tested at $Re = 7 \times 10^4$.

In comparison with Figure 2.5, a similar behavior can be observed; however, instead of an initial increase, a decrease is detected. While Figure 2.5, corresponding to square-base cylinders, shows a linear increase in the Strouhal number for angles of attack between 0° and 12° , Figure 2.10, for a circular-arc airfoil with 20% thickness, exhibits a linear decrease over the range from 0° to 25° . It is further observed that beyond 25° , the Strouhal number remains approximately constant at around 1.39.

On the other hand, agreement is found with the previously cited references for symmetric NACA 00XX aerodynamic profiles, in the sense that, as the angle of attack increases, the Strouhal number tends to remain constant. Up to this point, the behavior of a circular-arc airfoil under different angles of attack has been characterized. The question that arises is whether a similar behavior can be expected for a tall building immersed in the atmospheric boundary layer, where the curved building effectively behaves as a vertically oriented airfoil.

To address this, an additional series of wind tunnel tests was conducted using a scaled circular building model.

Aeroelastic Modeling

For the determination of wind-induced vibrations using wind tunnel testing, an aeroelastic modeling approach is employed. This approach depends on the complexity of the structural system and the external geometry. For most tall buildings, both the structural system and geometry exhibit the characteristic that the response is governed primarily by the fundamental lateral modes of oscillation, with significantly smaller contributions from higher-order modes and torsional modes. Therefore, it is generally sufficient to model only the two fundamental lateral modes. Furthermore, the mode shapes associated with the fundamental oscillation modes of tall buildings tend to be approximately linear. These conditions allow for the use of a simplified aeroelastic simulation technique, in which the building is modeled as a rigid body pivoted near its base. At the Boundary Layer Wind Tunnel Laboratory of the University of Western Ontario, it was demonstrated that this modeling technique adequately captures the most significant components of wind-induced dynamic responses (Davenport Wind Engineering Group, 2007) [8]. Scaling for this type of model is based on similarity theory. Provided that the essential properties of natural wind are reproduced in the wind tunnel—such as the mean velocity profile, turbulence intensities, and turbulence length scales— aeroelastic similarity can be achieved by modeling the building geometry at an appropriate length scale and maintaining equivalence between the following dimensionless parameters in both the model and the full-scale structure: density ratio, elastic force similarity and critical damping ratio.

In low-rise buildings or small structures, vibrations induced by wind action are generally negligible. However, in the case of large or tall buildings, wind effects become increasingly significant in terms of occupant comfort. Oscillations may occur which, although not structurally damaging, can be uncomfortable for occupants.

To prevent such issues and to properly assess wind effects on buildings, wind tunnel testing is employed to determine vibration characteristics. The Figure 2.12 presents a schematic representation of a two-degree-of-freedom aeroelastic model.

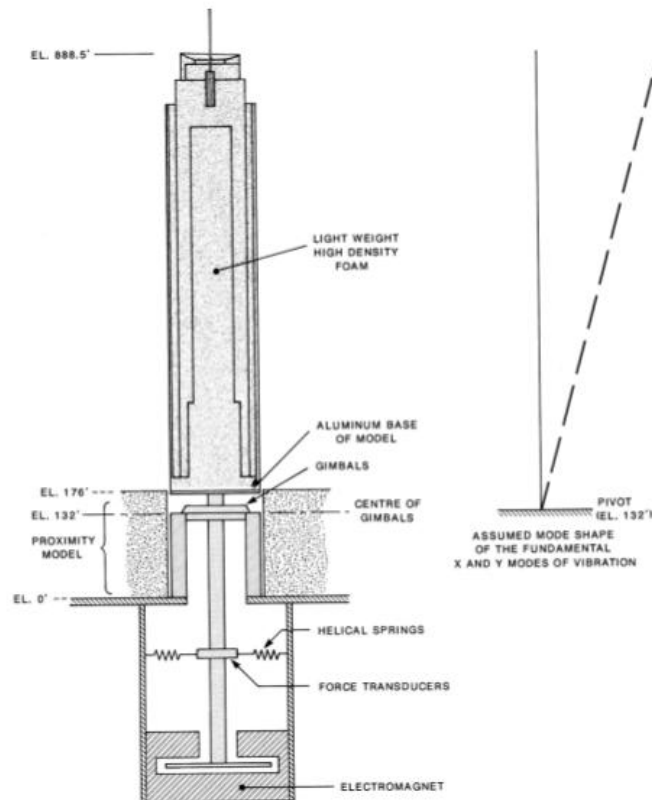


Figure: 2.12. Schematic of the model and measurement system.

To simulate the dynamic properties of the building in its fundamental lateral mode of oscillation, the tower is modeled as a rigid body rotating about a gimbal system, with a defined pivot point. Below this point, the building is considered a rigid body fixed to the base of the wind tunnel. From the lower part of the model, an aluminum rod passes through the gimbals and is supported by calibrated springs, which provide the required stiffness in the x and y directions. These springs are connected to force transducers equipped with electrical resistance strain gauges to measure deformations. Structural damping is provided by an eddy current device, whose current intensity can be adjusted to control the level of (electromagnetic) damping. The design of this type of model is based on the dynamic properties of the real building. Since the mode shapes are linear, the mass modeling of the structure is simplified by representing an effective mass moment of inertia with respect to the pivot point. Instead of using strain gauges to measure building displacement (through deformation measurements), the following alternative methods can be employed:

Displacement Measurement via Video Recording: in this method, a high-speed (slow-motion) camera is used to record the motion of the building model while it is subjected to simulated wind conditions. The recording allows direct observation of oscillations or vibrations induced by the wind. This technique enables the identification of vibration frequencies associated with the wind action.

Pressure Measurement in the Building Wake: in this method, pressure fluctuations are measured in the wake region behind the building, where the airflow becomes turbulent. By analyzing these pressure variations, the vortex shedding frequency generated by the interaction between wind and structure can be determined. This vortex shedding frequency is directly related to the building's vibration frequency, which helps identify potential resonance risks and supports design optimization to prevent uncomfortable or unsafe vibrations. This type of test corresponds to the one performed for the airfoil described in the previous section.

The Tests

The tests were carried out in the wind tunnel using the previously described building model. For the connection between the model body and the test base, polystyrene foam was used as both a fixation medium and a dynamic support. Tests were conducted using foams of different densities in order to identify the one that best represented the vibratory behavior of the full-scale prototype. This material enabled the simulation of the structural flexibility of the building and its dynamic response under wind loading, by adjusting the damping and stiffness

properties of the base. The optimal density was selected through preliminary free-vibration tests, comparing the observed oscillation modes with theoretical values obtained from numerical models. Once the most suitable configuration was determined, the foam was integrated into the wind tunnel mounting base, ensuring a stable connection while accurately reproducing fluid–structure interaction. This setup allowed for the evaluation of vortex shedding effects and the resulting vibratory response of the model.

Displacement Measurement via Video Recording

This method consists of a data acquisition system based on high-speed video recording and subsequent digital image processing to determine the vibration frequencies of the structure. The model was placed inside the wind tunnel and exposed to a flow velocity of 7 m/s, simulating real operating conditions. During the test, a high-speed camera with a sampling rate of 240 fps (frames per second) was used to accurately record the oscillations of the structure. In order to perform a detailed displacement analysis, a reference scale was included, allowing precise quantification of the movements observed in each frame. For data processing, the open-source software Tracker was used. This tool enabled the selection of a reference point on the structure and the tracking of its displacement over time. The software generated numerical data representing the motion of the selected point along the axis of interest, previously calibrated within the program. Since the accuracy of the analysis strongly depends on the selection of reference points and the quality of the recorded video, preliminary tests were conducted to optimize lighting conditions and image resolution, thereby minimizing potential measurement errors. The results obtained from Tracker were validated by comparison with manually extracted data through frame-by-frame analysis of the recordings. This manual validation allowed verification of the software accuracy and correction of possible discrepancies in displacement identification. Subsequently, the recorded data were exported in .txt format and processed using a custom MATLAB code, through which spectral analysis of the signals was performed. By computing the Power Spectral Density (PSD), the dominant frequencies associated with wind-induced oscillations were identified. Finally, the results were analyzed in relation to the structural parameters and the wind flow conditions in the tunnel. This procedure enabled an accurate characterization of the dynamic response of the structural model under wind loading, providing key information about its vibration modes. For both experimental methods, measurements were carried out using an angular sweep ranging from 0° to 25°. Initially, the model was positioned by aligning the arrows on its base with the 0° mark on the graduated ring, and the airflow velocity was stabilized at 7 m/s. Data acquisition was first performed at this initial position. Subsequently, the angular sweep was conducted in 5° increments. Each video recording had a duration of approximately 30 to 40 seconds.

III. RESULTS

The graphs presented below show the results obtained from the processing of the experimental data, as previously described in this study. The resulting curves allow visualization of the energy distribution of the flow as a function of frequency, highlighting the dominant peaks associated with vortex shedding. The red dashed lines shown in the graphs represent frequencies associated with the principal dimensions of the building and serve as a key reference for identifying potential structural resonance phenomena. The following graphs present the power spectra obtained from the displacement measurement tests using video recording, conducted at a wind speed of 7 m/s for angles between 0° and 25°. The three main frequencies in these spectra are clearly identified by red dashed lines.

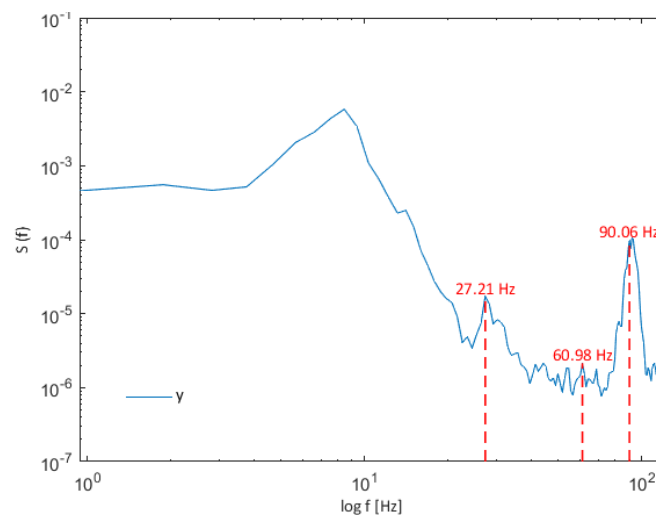


Figure: 3.1. Power Spectral Density. Video Test at 0°.

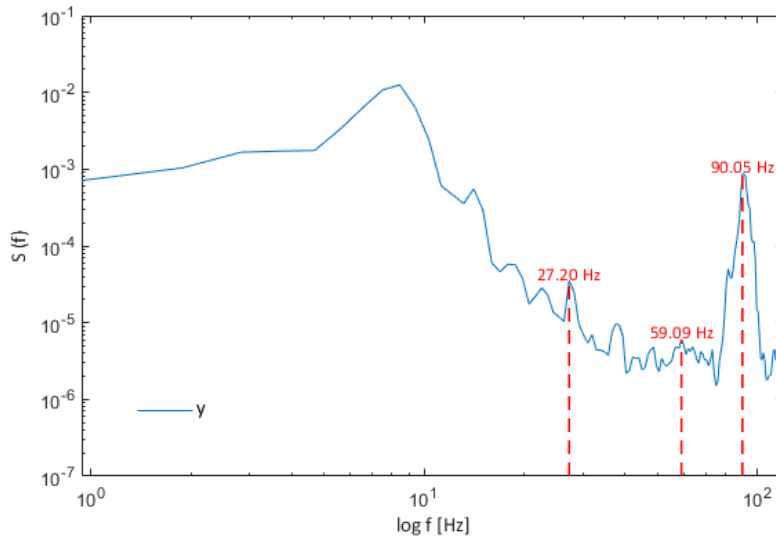


Figure: 3.2. Power Spectral Density. Video Test at 5°.

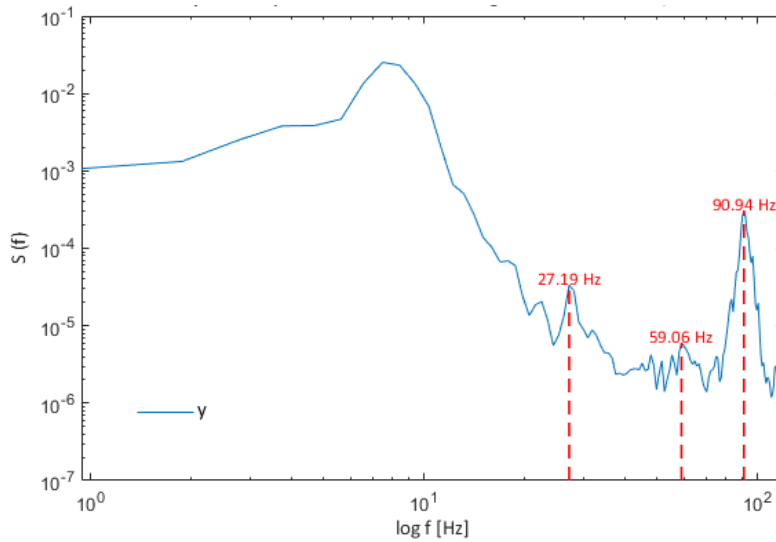


Figure: 3.3. Power Spectral Density. Video Test at 10°.

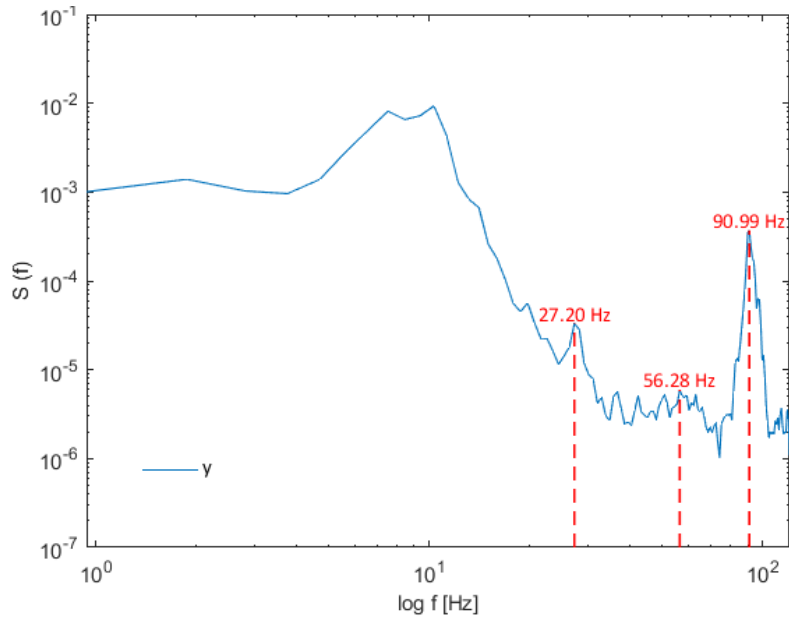


Figure: 3.4. Power Spectral Density. Video Test at 15°.

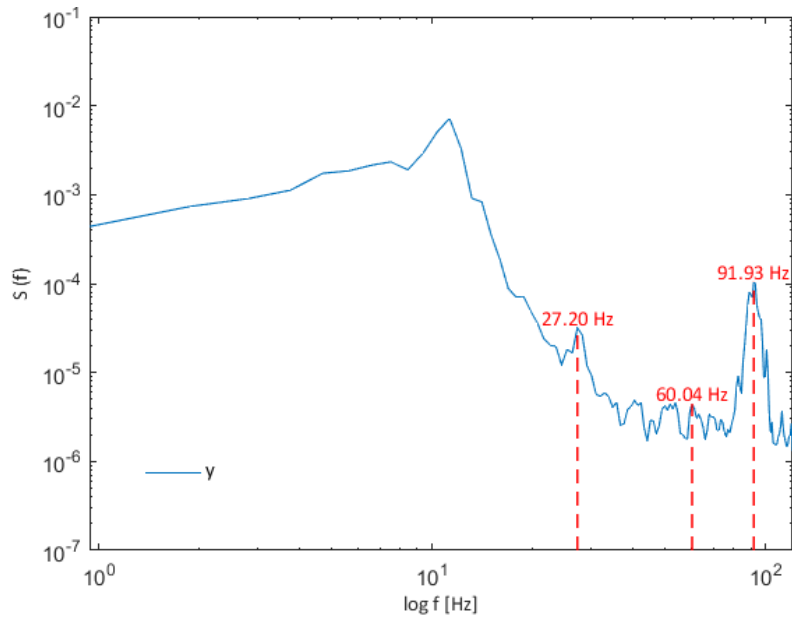


Figure: 3.5. Power Spectral Density. Video Test at 20°.

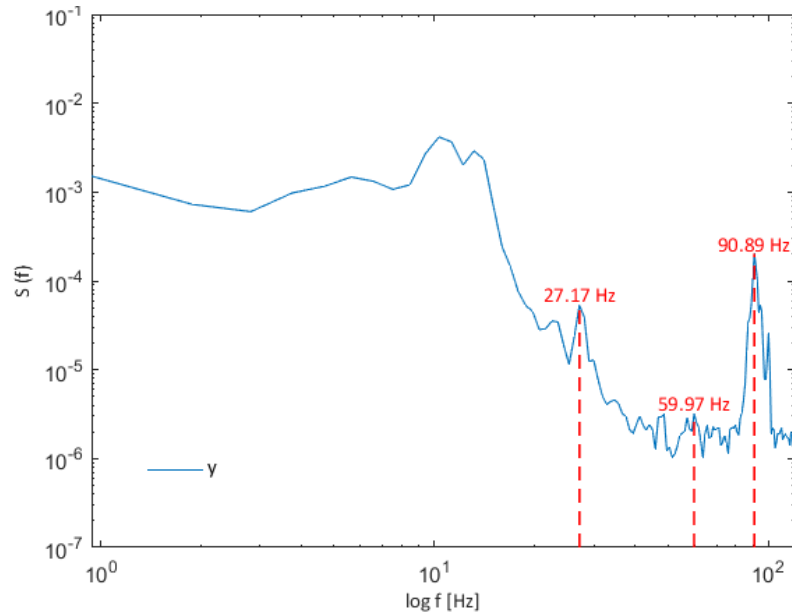


Figure: 3.6. Power Spectral Density. Video Test at 25°.

After a certain period, in a second stage, tests were conducted for angles of attack ranging from 30° to 90°, at intervals of 15°. Based on the video recordings and following the same procedure described previously, power spectral density plots as a function of frequency were obtained for 30°, 45°, 60°, 75°, and 90°, considering the three primary frequencies and including a fourth emerging frequency.

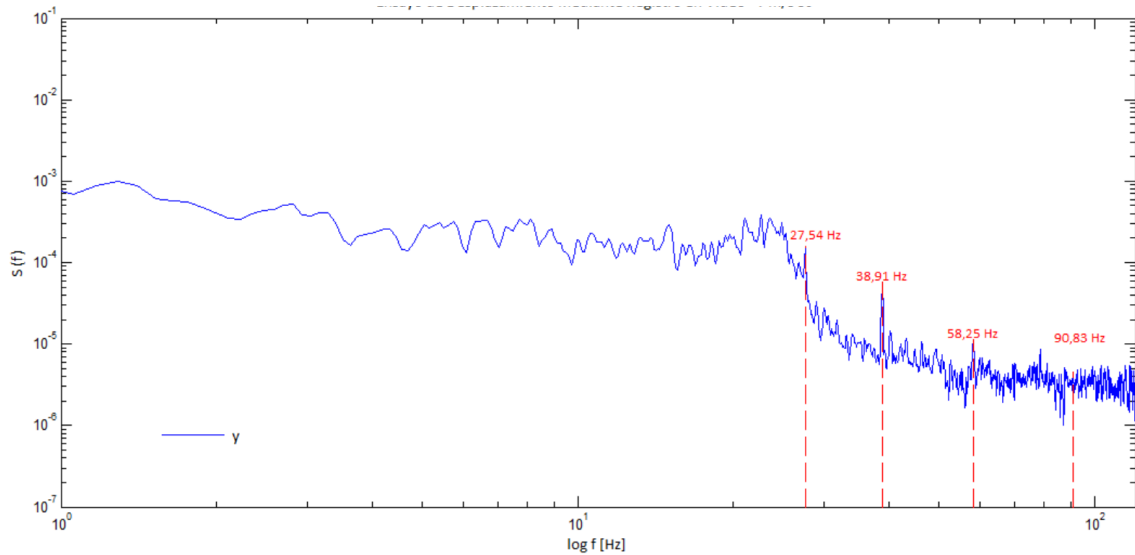


Figure: 3.7. Power Spectral Density. Video Test at 30°.

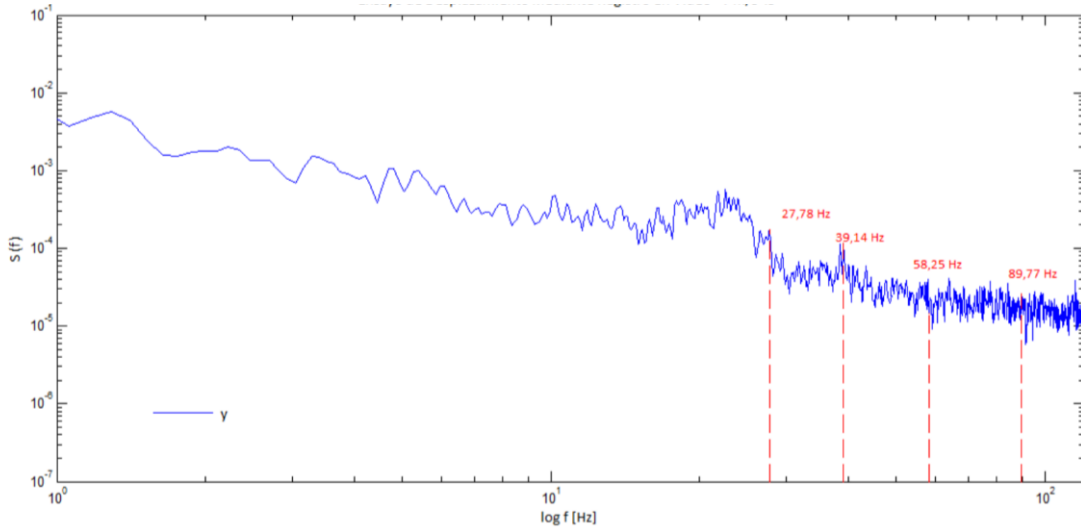


Figure: 3.8. Power Spectral Density. Video Test at 45°.

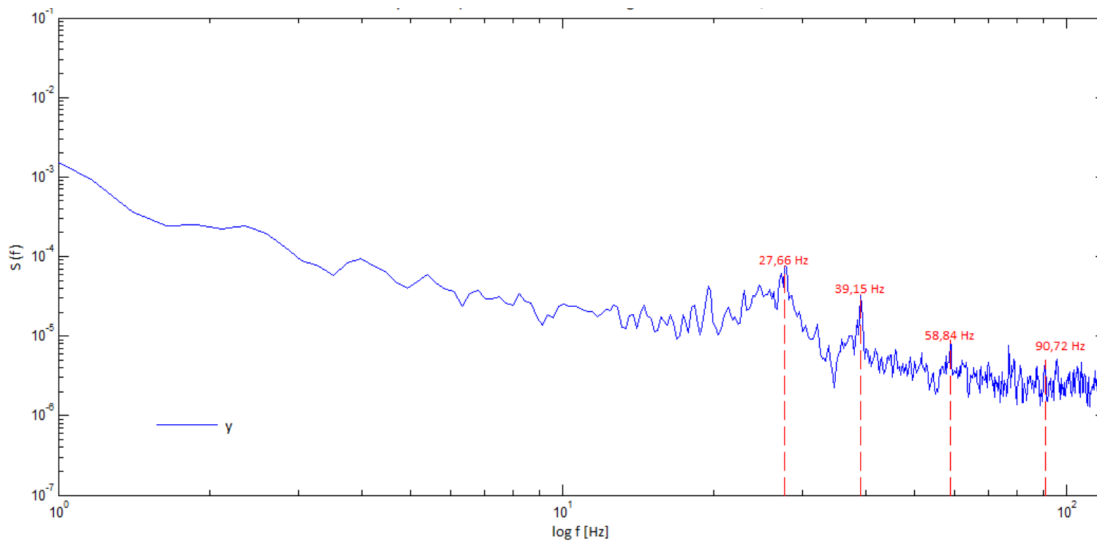


Figure: 3.9. Power Spectral Density. Video Test at 60°.

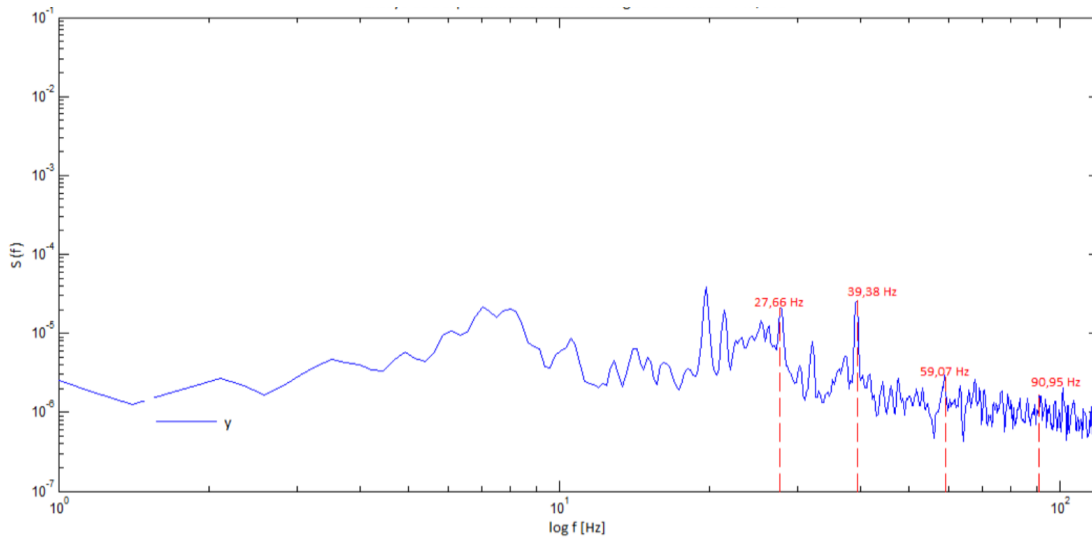


Figure: 3.10. Power Spectral Density. Video Test at 75°.

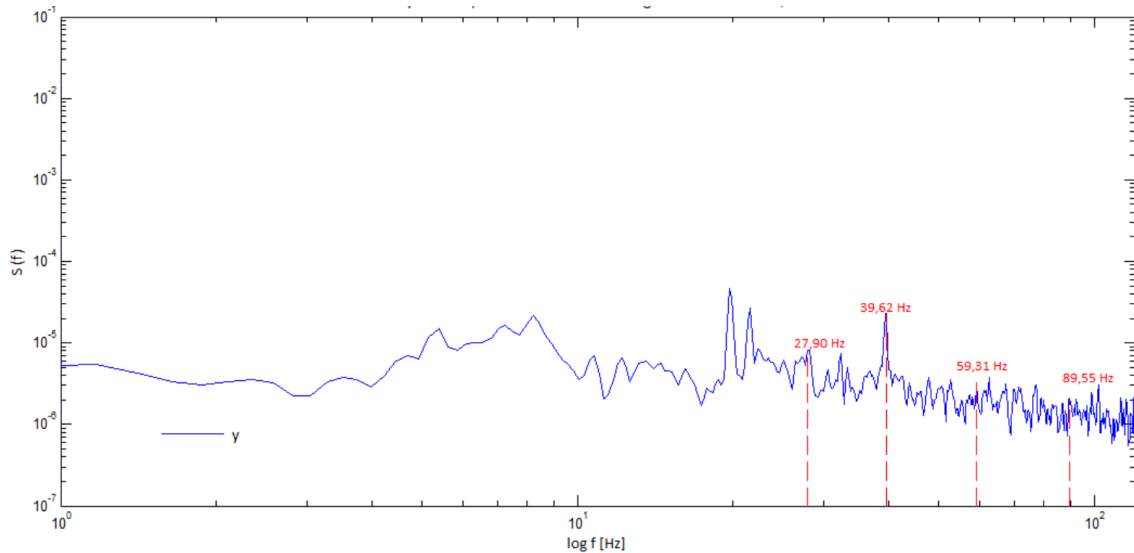


Figure: 3.11. Power Spectral Density. Video Test at 90°.

In all the analyzed cases, three dominant frequencies were identified, denoted as F1, F2, and F3, ordered from lowest to highest value. These frequencies are associated with the three principal dimensions of the building: height (F1), chord length (F2), and width (F3). For each of them, the corresponding Strouhal number was calculated over the range of tested angles of attack.

Frequency F3, located around 90 Hz, corresponds to the transverse vibration of the building. For angles of attack between 0° and 25°, it exhibits high energy ($\sim 10^{-4}$). However, beyond 30°, its energy decreases by approximately one order of magnitude. This indicates that, at low angles of attack, the curved building behaves similarly to an aerodynamic profile, shedding vortices in a comparable manner. Beyond 30°, however, the aerodynamic behavior transitions into stall, and the contribution of vortex shedding to lateral vibrations significantly decreases.

Frequency F2 (approximately 60 Hz), associated with the length of the building (corresponding to the chord of the airfoil of 0.12 m representing the curved structure), is of minor significance, as its energy remains nearly constant over the entire range of angles of attack.

Frequency F1, around 27 Hz, is associated with the height of the building model (0.24 m), and therefore with the along-wind (drag-related) response. Starting from an angle of attack of 30°, an additional frequency, F4 at approximately 39 Hz, emerges near this range. This frequency corresponds to a characteristic length of 0.18 m, representing approximately 72% of the model height.

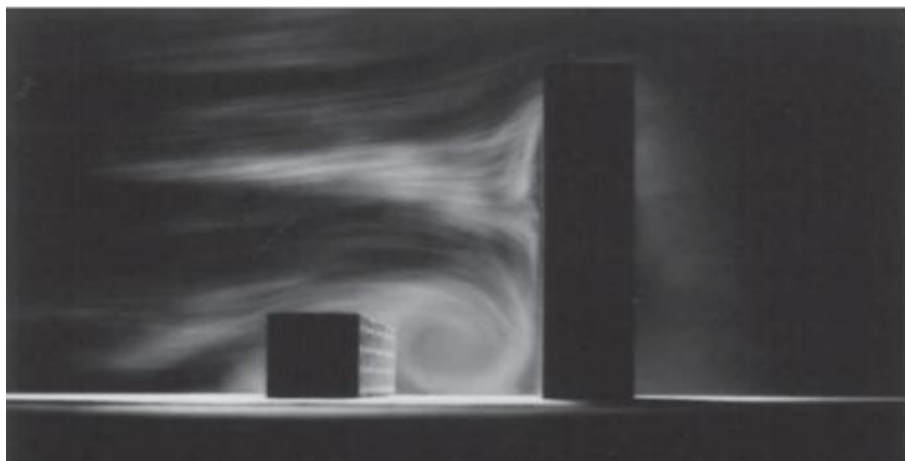


Figure: 3.12. Extracted from "Wind Effects on Structures", Cap. 15 "Wind-Induced Discomfort in and Around Buildings", pp. 231, de Emil Simiu y DongHun Yeo, (2019) John Wiley & Sons Ltd, UK [9].

In Figure 3.12, from the wind tunnel tests, it can be observed that the point of maximum wind impact on a tall building is located at approximately 72% of its height. Accordingly, the frequency of approximately 39 Hz is associated with a wavelength of 0.18 m, a value that coincides with 72% of the height of the building model tested in the wind tunnel. Therefore, as the building rotates up to 90° (flat plate position), a second frequency appears in the along-wind (longitudinal) direction. As a result, two frequencies act longitudinally on the structure: 27 Hz and 39 Hz. In Figure 3.13, the three main vibration frequencies (F1, F3, and F4) of the curved building model tested at a Reynolds number of 120,000 are presented. As can be observed, the Strouhal number for these vibrations remains nearly constant, indicating that it is independent of the wind angle of attack relative to the building. This finding is particularly significant, as for square-based buildings the Strouhal number exhibits variations at low angles of attack, then remains constant, and varies again at high angles of attack (see Figure 2.6).

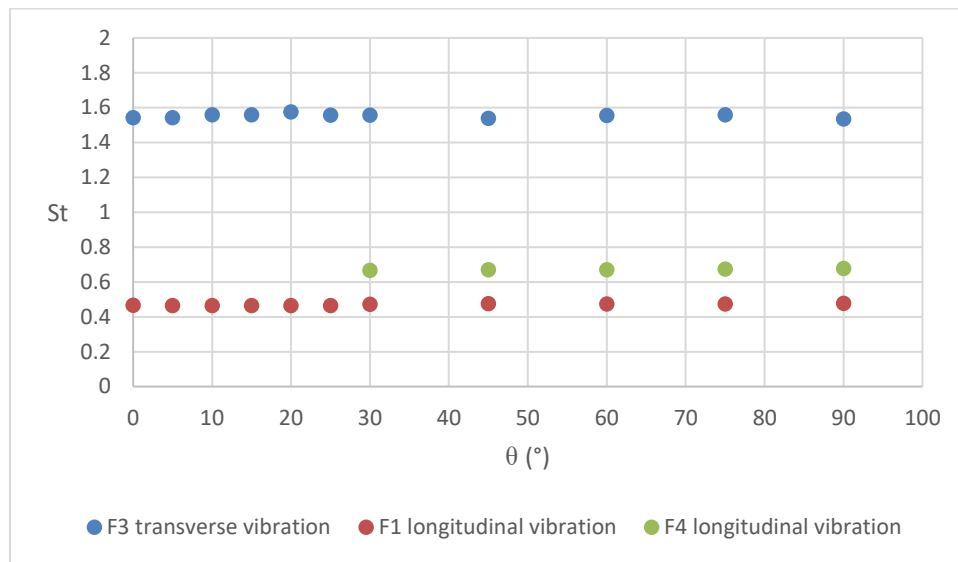


Figure: 3.13. Variation of the Strouhal number (St) with the angle of attack (α) for the two main vibration frequencies. Test at Reynolds number (Re) of 1.2×10^5 .

IV. CONCLUSIONS

The objective of this study was to determine the vortex shedding frequency and the associated Strouhal number. To this end, the aeroelastic response was measured through video recording and spectral analysis of displacements, aiming to identify the dominant vibration frequencies induced by wind action on the tallest curved building model ($h = 0.24$ m), and consequently, to determine the characteristic Strouhal number of this particular geometry.

The results show that, for a wind velocity of 7 m/s, the spectrum exhibits three families of peaks corresponding to the building model dimensions across all angles (0° to 90°): approximately 27 Hz, 60 Hz, and 90 Hz. In addition, a fourth frequency of 39 Hz appears from an angle of attack of 30° , associated with 72% of the model height. Among these, the frequency at 60 Hz, related to the building length or chord (0.12 m), is found to be negligible.

Regarding the frequency near 27 Hz, associated with the along-wind vibration and linked to the model height (0.24 m), a constant Strouhal number of approximately 0.47 is obtained throughout the entire range of angles of attack (0° to 90°).

The frequency of 39 Hz, which appears beyond 30° , also associated with along-wind vibration and related to the building height, yields a nearly constant Strouhal number of approximately 0.67.

Similarly, for the frequency of 90 Hz, corresponding to transverse vibration and associated with the model thickness (0.034 m), a Strouhal number close to 1.55 is obtained, remaining constant for all angles of attack.

Notably, this latter value is one order of magnitude higher than those corresponding to circular cylinders ($St \approx 0.20$) and rectangular prisms ($St \approx 0.18$), as reported in previous studies. The obtained Strouhal number is also consistent with the value reported in the referenced 2018 study for a curved roof with a 20% circular arc airfoil ($St \approx 1.4$).

These findings provide relevant experimental evidence for understanding the aerodynamic behavior of buildings with non-conventional geometries such as curved structures. Furthermore, the determination of the Strouhal number for this type of curved building—previously unreported in the literature—constitutes a novel experimental contribution.

REFERENCES

- [1]. Reglamento CIRSOC 102: Acción del Viento sobre las Construcciones, 2005.
- [2]. Meseguer, J., Sanz, A., Perales, J.M., Pindado, S., 2011; Aerodinámica Civil. Cargas de viento en las edificaciones; McGraw-Hill Profesional, ISBN 84-481-3332-3, Madrid, España.
- [3]. Knisely, C.W., 1990. Strouhal Numbers of Rectangular Cylinders at Incidence. A Review and New Data; Journal of Fluids and Structures pp. 4, 371-393.
- [4]. Yarusevych, Serhiy and Boutilier, Michael S. H., 2010; Vortex Shedding Characteristics of a NACA 0018 Airfoil at Low Reynolds Numbers; 40th Fluid Dynamics Conference and Exhibit; 28 June – 1 July 2010, Chicago, Illinois.
- [5]. Yarusevych, Serhiy, Sullivanand, Pierre E. and Kawall, John G.; 2009; On vortex shedding from an airfoil in low-Reynolds-number flows; J. Fluid Mech. Vol. 632, pp. 245-271.
- [6]. Md. Mahbud Alam, Y. Zhou, H. X. Yang, H. Guo and J. Mi (2010). The ultra-low Reynolds number airfoil waek; Exp. Fluids, pp. 48:10-103.
- [7]. Walter Carlos and Lässig Jorge, 2018; Analysis of Vortex Shedding Frecuencies, in Curved Buildings; IOSR Journal of Mechanical and Civil Engineering (IOSR-JMCE), Volume 15, Issue 6, pp. 62-68.
- [8]. Alan G. Davenport Wind Engineering Group, 2007; Wind Tunnel Testing: a general outline; The University of Western Ontario, Faculty of Engineering Science, London, Ontario, Canada.
- [9]. Emil Simiu and DongHun Yeo, 2019; Wind-Induced Discomfort in and Around Buildings; Wind Effects on Structures, JohnWiley & Sons Ltd, UK, Cap. 15, pp. 231.